CHARACTERIZATION OF DEFORMATION AND FRACTURE MECHANISMS OF WC-Co COMPOSITE USING HERTZIAN INDENTATION TECHNIQUE

Zhigang Zak Fang and Haibo Zhang
Department of Metallurgical Engineering, University of Utah
Salt Lake City, Utah, 84112, USA
Email: zak.fang@utah.edu

SUMMARY

In this research, mechanical behaviors of cemented tungsten carbide (WC-Co) material, which is a unique class of metal matrix composite with high volume fractions of reinforcements, were studied using the Hertzian indentation techniques. Under indentation load, macroscopic deformation of WC-Co was observed. The observed deformation is attributed to three microscopic mechanisms: the plastic deformation of the cobalt metal matrix, the plastic deformations of hard tungsten carbide (WC) particles and the formation of microcracks. A useful parameter, brittleness index, also obtained from the indentation test, was used to predict the mechanical behavior of WC-Co materials.

Keywords: quasi-plastic deformation, microcrack initiation, Hertzian indentation, tungsten carbide.

INTRODUCTION

Cemented tungsten carbide (WC-Co), which has a high volume fraction of reinforcement, is a unique class of metal matrix composite with hard brittle WC embedded in ductile metal matrix, usually the cobalt. Owing to its unique combinations of high modulus, strength, and moderate fracture toughness, cemented tungsten carbides (WC-Co alloys) are widely used for demanding applications. Its great technical and industrial importance has led to many extensive studies of their mechanical properties, including their deformation and fracture behaviors [1-2].

In general, cemented tungsten carbide materials are considered brittle materials. It is also widely recognized that WC-Co materials do have some degree of plasticity, especially under compressive loading. The mechanisms of plastic deformation of WC-Co materials are complex, and the behavior during deformation is not well understood. At present, there are two schools of thoughts pertaining to the plastic deformation of WC-Co materials during the fracture process [3]. One hypothesis is that only the binder phase is responsible for the plastic deformation of WC-Co composites. The second school of thought assumes that in the presence of a continuous carbide skeleton, the plastic deformation of the WC-Co composite would require considerable plasticity in the carbide phase, since the carbide skeleton would have to deform in continuum with the binder phase. However, in reality, the sensitivity of this kind of covalent material at

room temperature to abrupt brittle failure is so pervasive that even limited plasticity rarely occurs in ordinary stress-strain tests, not even in compression.

Hertzian contact testing with spherical indenters in normal loading on model flat structures is a special technique that may be used gain understanding of the mechanisms of deformation at a fundamental level. Recent studies using Hertzian indentation method have demonstrated that the plasticity is attainable not only in tough ceramics but also in WC-Co [4-5]. A principal advantage of the Hertzian indentation test is its capacity to reveal fundamental deformation-fracture properties in a highly controlled manner. In addition, simple analytic relations may be derived to correlate critical loads with basic material properties (modulus, hardness, toughness, and strength), and indenter radius [6].

In this study, the mechanical behavior of cemented tungsten carbide (WC-Co) was studied using the Hertzian indentation technique. The deformation mechanisms of WC-Co were interpreted based on the observation from the indentation test. Brittle index was measured and demonstrated that this parameter can be used to predict the mechanical behavior of WC-Co under the indentation load.

EXPEIMENTAL PROCEDURES

Sample preparation

Specimens were fabricated using conventional liquid-phase sintering techniques. After being cold pressed, the green parts were sintered in a vacuum furnace at 1400ºC for 60 minutes. Density values of the sintered parts were measured based on the Archimedes principle. Magnetic saturation and coercive force were measured to insure that the carbon balance and the metallurgical quality of the specimens met the usual requirements for these materials [7]. To evaluate microstructure, specimens were polished to 1 μm finish using diamond paste. Vickers hardness tests were conducted using a Vickers hardness tester (Leco, LV 700AT). The indentation load for hardness testing was 30 Kgf. All these measurements demonstrated that samples were fully dense and free of apparent defects.

Hertzian indentation

Hertzian indentations were made on the polished surfaces using a polycrystalline diamond (PCD) sphere of radius R equals 5.08 mm. This indenter is considered rigid relative to the specimen. Indentation tests were performed using a servohydraulic testing machine (MTS 810) with loads from 0.1 kN to 30.0 kN, loading rate was 100 N/sec.

Measurements of contact radius "a" at each given load P were taken within one hour after indentation. According to Johnson [8], although elastic recovery causes the depth, or the profile, of the residual impression to be different to that when fully loaded the radius of the contact impression remains virtually unchanged. Hence we can use the contact radius after unloading for the calculation. Using the measured contact radius, the indentation stress and strain were calculated using p_0 equals $P/\pi a^2$ and ε equals a/R respectively [9].

In order to study the nature of quasi-plastic deformation from the subsurface sections, one particularly useful technique—split and bond specimen—was used. The

details of this technique were referred to literatures [10-11].

P_C and P_Y measurement

To determine the load required to initiate quasi-plastic deformation, a mechanical profilometer (Tencor P-10) or an optical profilometer (Zygo, ZYGO Co.) was used to measure the axial displacement after the load was removed along the loading direction after each load increment. When the axial displacement reached a preset value, the corresponding load was designated as the critical load for the onset of quasi-plastic deformation. In this study, the onset of plastic deformation was detected when the measured depth was greater than the amplitude of the background signals, which were caused by the surface roughness of the specimen. To determine the load required to initiate fracture, the specimen was indented with incremental load. The specimen was examined using a light microscope after each indentation. The load at which about a quarter of a full circle of the ring crack was visible was designated as the critical load for formation of ring cracks. In order to obtain the accurate value of P_C and P_y, at least five points of measurement were taken to obtain an average.

RESULTS AND DISCUSSION

1. Indentation stress-strain curve

After each indentation test, surface damage in the form of indentation impressions was observed using an optical microscope. As shown in Figure 1, when the indentation load was below a certain threshold value, the "sink in" phenomenon was observed. When the load exceeded a threshold value, in addition to the "sink in", ring cracks and even radial cracks were found.

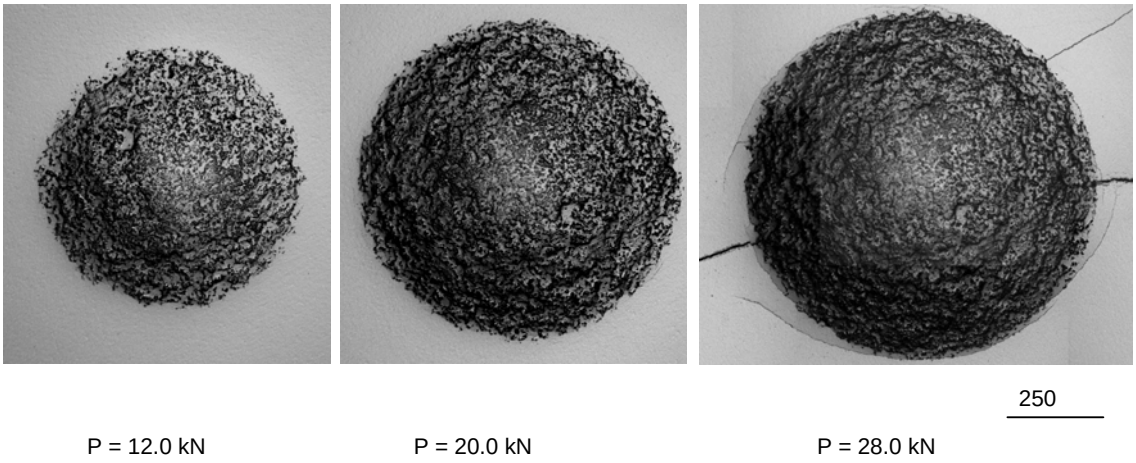

Figure 1 Indentation impressions at different indentation loads.

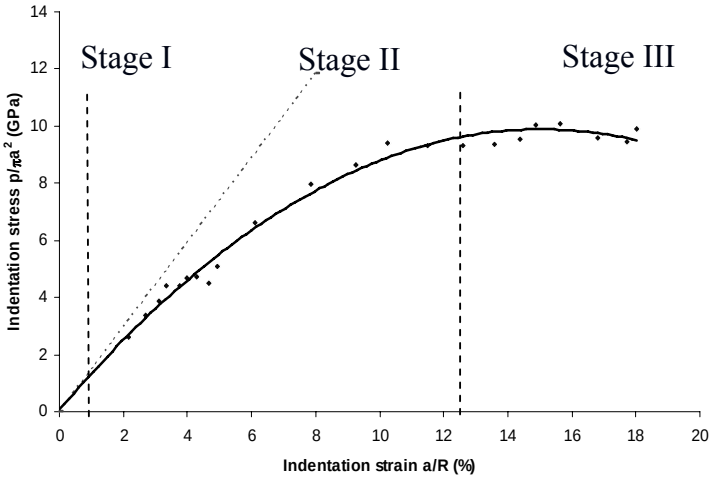

Figure 2 Hertzian indentation stress-strain curve of WC-10wt%Co, data were taken with polycrystalline diamond indenter. Indenter radius R = 5.08 mm.

Using the indentation load versus contact radius data, indentation stress and strain data can be calculated and plotted as a stress-strain curve as shown by Figure 2. Each data point represented one experimental indentation, while the solid line was a numerical regression fit of the data. In order to fully characterize the process from deformation to fracture, the stress-strain relationship of WC-10wt%Co is divided into three stages: initial elastic, elastic-plastic, and fully plastic.

1.1 Initial elasticity

At the initial application of load, the response was elastic and can be predicted from Hertz relation by equation (1). The inclined straight dash line through the origin was the calculated perfect elastic response using the Hertzian relation as shown by the following equation [12].

$$P_m = \frac{3E}{4\pi k}\frac{a}{R} \tag{1}$$

Where P_m is the mean contact pressure, E is Young's modulus, a the contact radius, R the indenter radius, and k is a dimensionless constant given by

$$k = \frac{9}{16}\left[\left(1-\nu^2\right)+\left(1-\nu'^2\right)\frac{E}{E'}\right] \tag{2}$$

where ν and ν' are Poisson's ratios, and E and E' are Young's modules of the specimen and indenter respectively. Equation (1) assumes linear elasticity and makes no allowance for yield within the specimens.

1.2 Elastic-plastic

As the indentation strain increases, the indentation stress-strain curve deviates from a linear relationship, indicating a "yielding" behavior. Above the yield point, the indentation stress continues to increase monotonically with indentation strain, exhibiting an "apparent strain hardening" behavior. At high strain values, the indentation stress

levels off, even though the strain continues to increase. In order to understand the mechanisms of the nature of the plastic deformation, the split and bond samples were analyzed.

Figure 3 shows the subsurface damage, i.e., the plastic zone observed from the split and bond sample. In Figure 3, the upper part is the top view of one of the two halves of the bonded specimen, while the lower part is the side view of the same half sample. It appears that the plastic zone has a semi-spherical shape with its diameter smaller than that of the contact circle.

An enlarged view, shown in Figure 4, was taken from the heavily damaged zone in Figure 3. It showed that there were a substantial number of microcracks in the specimen at larger indentation loads. These microcracks follow several crack paths in the microstructure: transgranular cracks through WC grains, intergranular cracks along WC/WC grain boundaries, and cracks along the WC/Co interfaces. A substantial number of slip bands were observed within the WC grains, distributed in the entire plastic zone. This observation demonstrates that deformation of WC grains by slip contributes in part to the overall observed deformation of WC-Co.

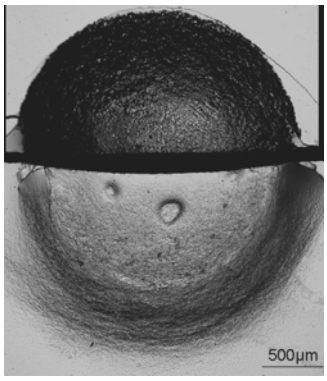

Figure 3 Plastic deformation zones in the subsurface of the split-bond specimen.

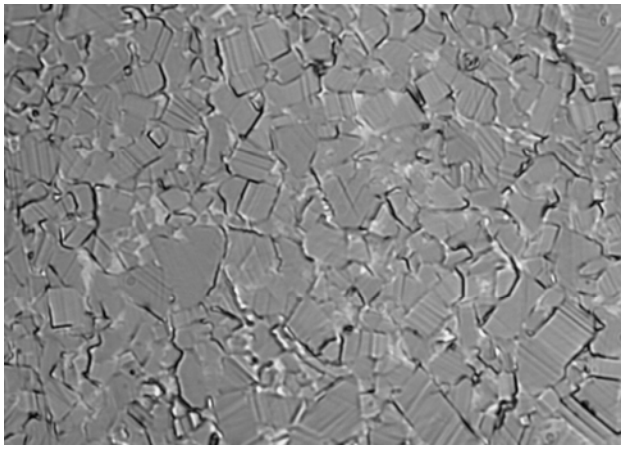

Figure 4 Enlarged view of subsurface microcracks in heavily damaged area in Figure 3.

Although it is not visible in the micrographs, another contributing process to the overall deformation of WC-Co is the cobalt phase. In general, the plastic deformation of Co in the WC-Co composite can be accomplished by the slip of cobalt or the Martenstic transformation from fcc to hcp [13-14].

In short, macroscopically, during the second stage of the indentation stress-strain curve, indentation stress-strain curve deviates from the Hertzian elastic relation and the WC-10wt%Co composite experience quasi-plastic yielding and apparent strain hardening. Microscopically, WC grains plastically deform in continuum with the binder phase. Microcracks form to accommodate the continuous deformation without macrocracks.

1.3 Full plastic

The last stage of the indentation stress-strain curve is the fully plastic stage. Microscopically, the skeleton of WC was broken up and substantial number of microcracks formed, also shown in Figure 4. These microcracks were frequently at the WC/WC boundary, while some of them were at WC/Co interface. The high percentage of WC/WC microcracks is an indication that the WC skeleton has been damaged. The number of microcracks along the WC/Co interfaces also continued to increase as the indentation strain increased during fully plastic stage. The microcracks initiated when the local binder phase reached the limit of its accommodation of deformed WC phase.

2. Brittleness index

The experimental results described above show the behavior of WC-Co composites when loaded with spherical indenters, undergo elastic and quasi-plastic deformation, formation of micro-cracks beneath the contact area, and eventually formation of ring cracks or radial cracks. There are critical points associated with the onset of the quasi-plastic deformation (P_Y) and the ring cracks or radial cracks at large load (P_C). In order to represent the relative propensities of a material for quasi-plastic deformation or forming ring cracks, Rhee et al [15] introduced the concept of a brittleness index given by P_Y/P_C. Because both P_Y and P_C can be measured using the indentation tests, the brittleness index P_Y/P_C can be experimentally determined.

Table 1 lists the measured values of P_Y and P_C and the calculated value of the brittleness index P_Y/P_C. As expected, the brittleness index increases with the increase in hardness. The relationships between the brittleness index and other intrinsic mechanical properties are, however, more complex. For brittle materials, Frank and Lawn derived [16] an expression of the critical load of cone crack P_C as:

$$P_c = A\left(\frac{K_{IC}{}^2}{E}\right)R \tag{3}$$

$$A = \frac{4\pi^2 k}{3I_*{}^2} \tag{3a}$$

where k is from equation (2), I_* is a dimensionless integral related the stress intensity factor from the tensile stress field at the contact circle, K_{IC} the fracture toughness, E the Young's modulus of the specimen, and R the indenter radius.

Table 1 Measured mechanical properties and critical loads for ring crack and the onset for yielding of a group of WC-Co.

Sample No.	Hardness (H_{V30})	K_{IC} (MPa $m^{1/2}$)	P_C (kN)	P_Y (N)	BI (10^{-3})
1	1361.8	13.71	12.3	90	7.32
2	1422.2	12.91	10.5	100	9.52
3	1524.6	10.94	10.5	110	10.48
4	1315.0	14.09	13.0	70	5.38
5	1375.4	12.82	16.0	90	5.63
6	1443.0	12.42	15.0	100	6.67
7	1139.2	17.41	25.5	50	1.96
8	1214.4	15.34	25.5	60	2.35
9	1256.6	14.87	25.0	70	2.80
10	1061.5	19.03	29.0	40	1.38
11	1113.6	18.01	26.0	50	1.92
12	1112.9	17.08	25.0	50	2.00
13	998.9	19.93	29.0	40	1.38
14	1016.9	18.45	26.0	40	1.54
15	1028.8	17.70	29.5	50	1.69
16	1172.2	13.62	21.0	60	2.86

For the same material, the threshold load for quasi-plasticity is given by [17]

$$P_y = D\left(\frac{H^3}{E^2}\right)R^2 \tag{4}$$

$$D = \left(\frac{1.1\pi}{c}\right)^3\left[\frac{3\left(1-\upsilon^2\right)}{4}\right]^2 \tag{4a}$$

where c is a "constraint factor" from the simple relation between indentation hardness and material yield stress, $H = cY$. v is the Poisson ratio of indented material, H is the

indentation hardness of the tested material, E Young's modulus; and R the indenter radius. Equation (4) shows that the relationship between critical load and indenter radius is quadratic.

Combining Equations (3) and (4) gives the expression for the brittleness index as a function of the modulus, hardness, and fracture toughness of a material:

$$\psi = \left(\frac{P_y}{P_c}\right) = \left(\frac{D}{A}\right)\left(\frac{H}{E}\right)\left(\frac{H}{K_{IC}}\right)^2 R \qquad (5)$$

If Ψ less than 1, the material responds quasi-plastically; if Ψ greater than 1, the material responds in a brittle fashion. In other words, the brittleness index is a parameter that considers the combined effects of the strength, fracture toughness, and the loading condition of a material, which may have better correlation with the real life mechanical behavior of the material.

In order to obtain further insight into the merit of the brittleness index parameter, the measured data points of the brittleness indices of a group of specimens as listed in Table 1 are also included in the figure 5. For comparison, plot of the K_{IC} versus Hv is also shown in Figure 5. It can be seen that, although Ψ is proportionally related to the hardness, the relationship is nonlinear. The sensitivity of the changes of Ψ vs. Hv is greater at the higher Hv ranges. In contrast, the relationship between K_{IC} and Hv is close to linear. It is believed that the differences between Ψ and K_{IC} and their correlations with Hv can be understood based on the propensity of the material to either quasi-plastically deform or form ring cracks. It appears that the brittleness index is a more sensitive parameter for judging the response of WC-Co composites to indentation loading. When the brittleness index is high, the material will form ring cracks. When the brittleness index is low, quasi-plasticity will be more prevalent.

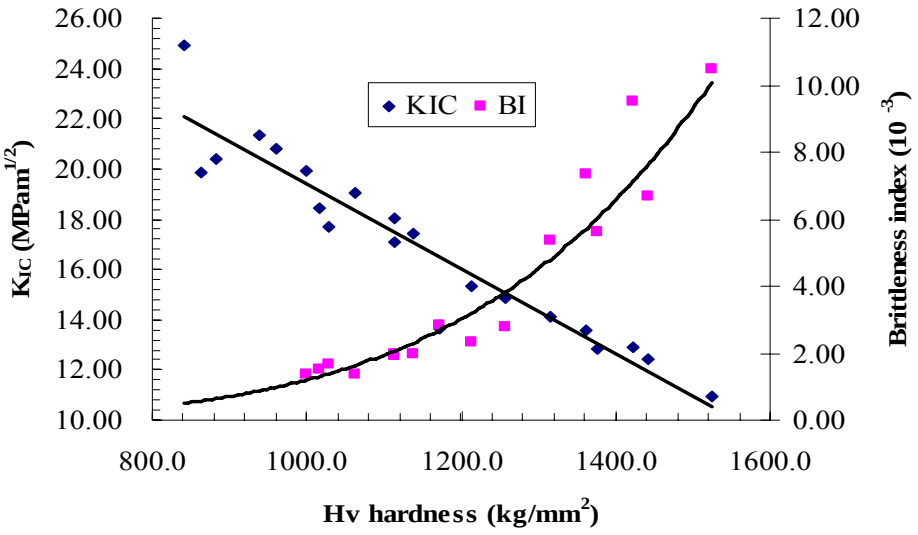

Figure 5 Measured brittleness index versus hardness of a group of WC-Co specimens. Polycrystalline diamond indenter, radius R = 5.08mm.

Further, the brittleness index is not only a material-dependent parameter, is also a function of the radius of the indenter. When the radius of the indenter is large, the brittleness index of the material will be higher. This suggests that, for the same material with constant hardness and fracture toughness values, the response of the material to indentation loading will vary depending on the radius of the indenter. When a larger indenter is used, materials will respond in more brittle fashion, while when a smaller indenter is used, the material will respond in less brittle fashion, i.e., with more plasticity. This analysis has important implications to practical application of these materials.

CONCLUSION

The Hertzian indentation method was used to study the plastic deformation and fracture behavior of cemented tungsten carbide loaded with a spherical indenter. The quasi-plastic deformation of homogeneous WC-Co material was analyzed in three separate stages: initial elastic, elastic-plastic, and fully plastic deformations. The mechanism of the quasi-plastic deformation of WC-Co composites involves the formation of microcracks, especially in the higher indentation strain range.

The propensity of the WC-Co material to either form ring cracks or undergo quasi-plastic deformation can be evaluated based on its brittleness index. The brittleness index is a function of not only the material properties but also the radius of the indenter with which the indentation load is applied.

REFERENCES

[1]B. Roebuck and E.A. Almond. *International Materials Research*, 1988, Vol.33, No.2, pp. 90-110

[2] L.S. Sigl and H.F. Fischmeister. *Acta metall*., 1988, Vol. 36, No. 4, pp. 887-897

[3]Gopal S. Upadhyaya. *Cemented Tungsten Carbides Production, Properties, and Testing* (Noyes Publications, 1998).

[4]F. Guiberteau, N. P. Padture and B. R. Lawn. *J. Am. Ceram. Soc.,* 1994, Vol. 77, p. 1825.

[5]H.Zhang, ZZ. Fang and J. Belnap. *Metall Trans A,* 2007; 38A, pp. 552-61.

[6]B. Lawn, Y. Deng and V. Thomson. *J Prosthet Dent* 2001, 86, pp.495-510.

[7]Z. Fang and J. W. Eason, *The International Journal of Powder Metallurgy*, 1993, Vol. 29, No. 3, pp. 259-265.

[8]K. L. Johnson, *Contact Mechanics*, Cambridge University Press, Cambridge, 1985.

[9]H. Chai and B. R. Lawn, *Acta Mater.*, 2002, Vol. 50, pp. 2613-2625.

[10]H. Zhang and ZZ Fang. *Int. J. Refractory Metals & Hard Material.* 2008; 26, pp.106-14.

[11] H. Cai, M. S. Kalceff and B. R. Lawn, *J. Mater. Res*., 1994, Vol. 9, No. 3, pp. 762-770.

[12] B. Lawn and T. Wilshaw. *J Mater Sci.,* 1975;10, pp.1049-81.

[13]B. Roebuck and E. Almond. *Int Mater Rev.,* 1988;33, pp.90-110.

[14]U.Beste U, E. Coronel and S. Jacobson. *Int J Refrac Met Hard Mater.,* 2006; 24, pp.168-76.

[15] Rhee, Young-Woo, Kim, Hae-Won, Y. Deng and B. Lawn. *J. Am. Ceram. Soc.,* 2001, Vol. 84(5), pp. 1066-1072.

[16] F. Frank and B. Lawn. *Pro Roy Soc London.,* 1967;A299, pp.291-306.

[17] B. Lawn. *J Am Ceram Soc.,* 1998;81, pp.1977-94.

Previous Paper **Back to Programme** **Back to Topic** *Next Paper*